Practical test of a point-source integrating cavity absorption meter: the performance of different collector assemblies

Rüdiger Röttgers, Wolfgang Schönfeld, Peter-Rüdiger Kipp, and Roland Doerffer

A prototype point-source integrating cavity absorption meter (PSICAM) is presented and compared with spectrophotometric absorption measurements. Different light collector assemblies of the PSICAM were tested regarding their capability to determine the absorption of water constituents accurately over a wide range of concentrations and scattering properties. The PSICAM setup with a radiance-type sensor showed the best performance. It was compared with a photometric absorption determination using nonscattering dye solutions. The mean difference between both methods was less than 2.4% in the spectral range of 400–700 nm. The absorption determination with the PSICAM, when equipped with a radiance sensor as a light collector, was only little affected by scattering and temperature. We conclude that the PSICAM can be used to determine the absorption of natural seawater samples at ambient temperatures.

OCIS codes: 010.4450, 120.3150, 120.4640, 300.1030.

1. Introduction

The determination of light absorption coefficients in natural water is of great interest for many scientific questions. For example, biological oceanographers are interested in the amount of light absorbed by planktonic algae to quantify primary production or use spectral information of the absorption to identify different taxonomic groups of planktonic algae by its specific absorption characteristics, which results from differences in their cellular pigment composition. Bio-optical oceanographers need information of the absorption coefficient to quantify the different components of the water constituents, e.g. gelbstoff, and to use this information for remote sensing applications.

Methodologically it is difficult to measure absorption coefficients accurately without the influence of scattering by the water and on particles. A few *in situ* instruments were designed and have been recently used to measure absorption and scattering in the water column,[1,2] such as the AC-9 (WETLabs, Oregon). Using a laboratory photometer, the particulate absorption by planktonic algae is determined by placing a relatively dense algal suspension in a cuvette in front of an integrating sphere, which collects most of the forward-scattered photons.[3] At lower natural algal concentrations, the algae are concentrated onto a filter (filter pad method) and then measured similarly.[4,5] For all three methods the photon loss by backscattering has to be corrected.[4,6] To also collect the backscattered photons, a better but rarely used solution is to place the sample in the center of the integrating sphere.[7,8] When the filter pad method is used, we have to consider that multiple scattering in the filter increases the optical path length. The amplification factor has to be known to convert the measured absorption of the particles on the filter to the absorption coefficient of the particles in suspension. For the commonly used glass fiber filters, this factor is theoretically 2.[9] But empirical determination of this factor by several authors using algae cultures[4,10–12] showed that it is a major source of uncertainty when the absorption by particulate matter is determined in natural waters.

One method to avoid or reduce the adverse effects by scattering is to fill the water sample directly into an integrating sphere. This was first suggested by Elterman[13] and later adopted for measurements of

The authors are with the Institute for Coastal Research, GKSS Research Center Geesthacht, Max-Planck-Strasse 1, D-21502 Geesthacht, Germany. The e-mail for R. Röttgers is rroettgers@gkss.de.

Received 3 December 2004; revised manuscript received 1 April 2005; accepted 5 April 2005.

0003-6935/05/265549-12$15.00/0

seawater by Fry and co-workers.[14,15] The first versions of integrating cavity absorption meters had cylindrical forms. Later Kirk[16] suggested a spherical form for the cavity, which simplifies the theoretical description and calculations. The cavity should be illuminated from outside, like the former versions. This design caused problems in manufacturing since it comprises an inner cavity, which holds the water sample, and an outer cavity, which is used to provide a homogeneous illumination of the inner one. In search of a simpler design, Kirk[17] proposed a cavity that is illuminated by a central light source: the point-source integrating cavity absorption meter (PSICAM). Recently the first prototypes were developed and the necessary theoretical analyses were performed.[2,18]

In this paper we show the first results obtained with a PSICAM developed at the GKSS Institute for Coastal Research. Different setups of the light collector assembly have been proposed by Kirk,[17] by Leathers *et al.*,[18] and by the authors of this paper. The properties of these different setups were compared by determining the accuracy of the absorption measurement for a set of samples over a wide range of absorption and scattering. Furthermore, the best-performing setup was tested for the influence of temperature on the absorption determination. The results for nonscattering samples were compared with absorption measurements using a spectrophotometer.

2. Material and Methods

A. Point-Source Integrating Cavity Absorption Meter

The integrating cavity of our PSICAM [Figs. 1(a) and 1(b)] has an inner diameter of 9.50 cm and was made out of a block (edge length of 12 cm) of a diffuse reflective plastic material (OP.DI.MA., Gigahertz-Optik, Germany) that has properties similar to Spectralon (Labsphere Inc.). The reflectivity of this material depends on the material thickness (97% and 98% for a thickness of 10 mm). To simplify its manufacturing, the raw material surface was used without any additional coating of the inner cavity surface. This surface is water repellent, and problems with contamination by natural soluble substances could not be observed when river water was used with a high gelbstoff concentration. Particulate matter can easily be washed out of the cavity (but see below for the nigrosine solution used). The block is covered with a thick aluminum foil to prevent any light entering the sphere from outside. The central light source consists of a small scattering sphere made of Teflon (DuPont) with an outer diameter of 12.0 mm. The cavity has two openings that can be closed by Teflon stoppers. One is for inserting and changing the central light source, and one is for filling and emptying the cavity. Light is provided by an electronically stabilized 150 W halogen bulb (LQ 1700, Fiberoptic-Heim, Switzerland). A conversion filter (FG3, Schott, Germany) is used to reduce the high emission in the red and near-infrared spectral range, giving a more

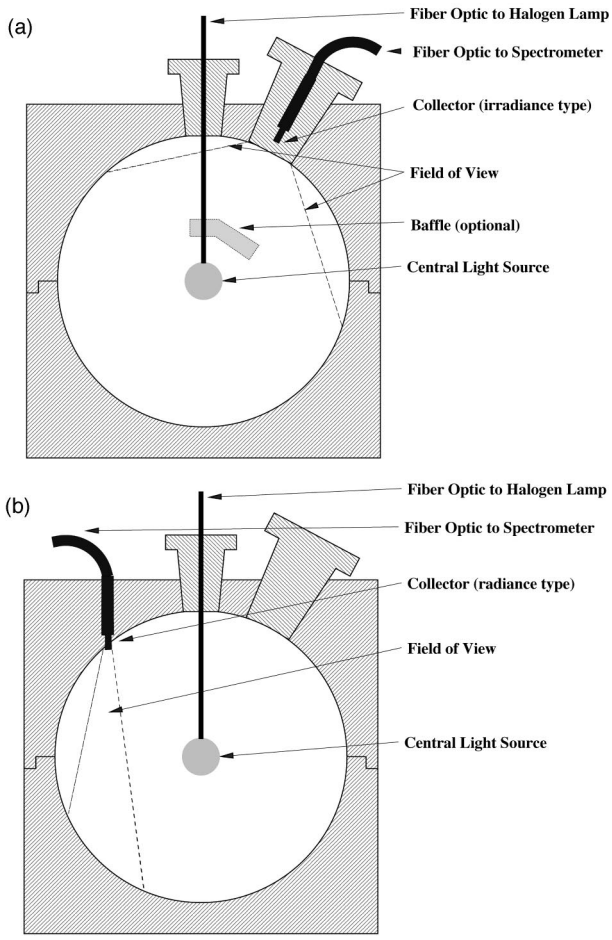

Fig. 1. Cross sections of the PSICAM prototype with different collector assemblies. (a) Irradiance-type light collector with or without a baffle as used in setup I and IS, respectively. (b) Radiance-type collector of setup R.

equal radiation over all used wavelengths (Fig. 2). The resulting light beam is guided to the central diffuse emission sphere by a quartz-glass fiber bun-

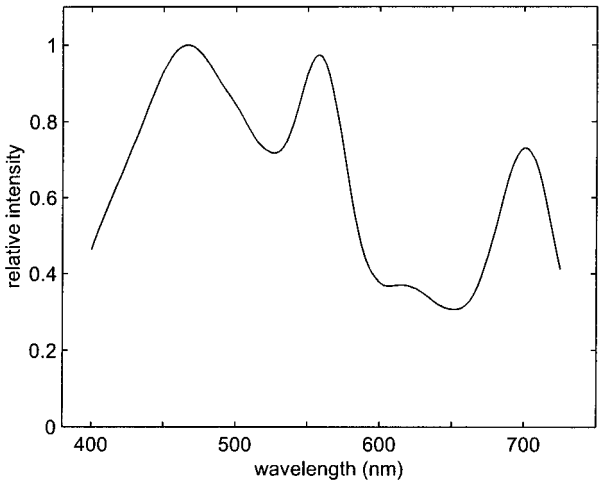

Fig. 2. Normalized spectral response of the light source and the detector measured in the PSICAM filled with purified water.

dle. That part of the fiber bundle, which sticks into the cavity, is enclosed in a 10 cm long steel tube (diameter of 3.0 mm) and carries at its end the emission sphere. A Ramses-ACC UV–visible spectroradiometer (Trios, Germany) is used as the light detector. It includes a photodiode array that covers the spectral radiation from 300 to 725 nm with an interval of 2.5 nm.

Another quartz-glass fiber bundle guides the light from the cavity to the detector entrance. The light collector at the end of this fiber bundle is designed in three different ways: In setup I the end of the fiber optic is covered by a Teflon window and is directed toward the central light source [Fig. 1(a)]. Here the detector acts like an irradiance sensor collecting light from all directions inside the cavity; this is the original setup by Kirk.[17] In setup IS, photons coming directly from the central light source are prevented from being collected by the irradiance sensor by inserting a baffle plate made out of Teflon (thickness of 8 mm) between the central light source and the irradiance detector [Fig. 1(a)]. With this setup only photons are collected that are scattered at particles or at the cavity wall. The design prevents the cuvette from becoming a beam attenuation meter for samples with a high absorption coefficient. In the third setup, R, the collecting fiber optic enters the integrating cavity through a small hole (diameter of 3.1 mm) parallel to the steel tube holding the central sphere [Fig. 1(b)]. Without a diffuser the fiber has only a narrow field of view and thus does not directly collect any light coming from the central light source. In this setup the detector acts like a radiance sensor. It measures the light reflected at the cavity wall opposite to the collector as well as the path radiance, i.e., the light scattered into the receiving cone of the collector. This setup was proposed by Leathers *et al.*[18] and also by Kirk[19] (as an alternative to his original setup). Small problems can occur because the detector collects light coming from the cavity wall directly. Including a small sampling cavity, as Pope and Fry[20] did to measure the real wall radiance, would not improve the detector response for the PSICAM since this cavity would always see direct light from the central light source. The setup of Pope and Fry did not have this problem, since their cavity is illuminated from outside. Before the PSICAM could be used for regular measurements, possible problems caused by the long-term stability of the halogen lamp and by fluorescence of substances in the sample had to be investigated.

B. Stability of the Halogen Light Source

Figure 3 shows the relative changes of the illumination by the halogen lamp over a period of 5 h at different wavelengths. The lamp was turned on 1 h before the start of the experiment. The total differences due to changes of the lamp output and/or the spectroradiometer response are less than 1.3% over the whole period, i.e., less than 0.3%/h. A transmission measurement is made within 2 min; hence the error due to alterations of the lamp output and the spectroradiometer response can be considered as negligible.

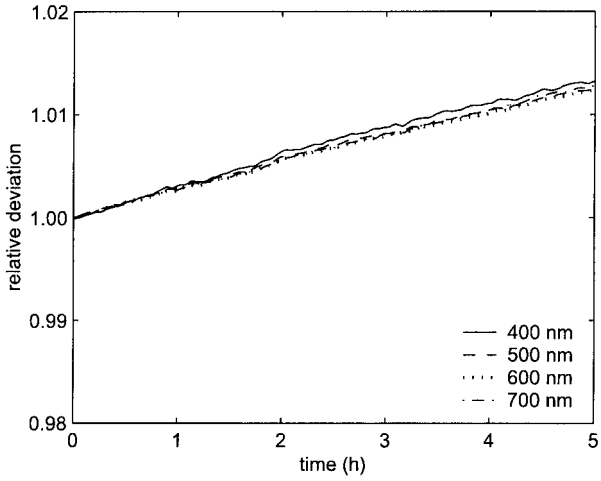

Fig. 3. Normalized deviation of the halogen light source measured with the spectroradiometer for different wavelengths over a period of 5 h. The lamp and the radiometer were switched on 1 h before the start of this experiment.

C. Influence of Sample Fluorescence

Since the PSICAM is illuminated with white light and not monochromatically, it has to be analyzed if any fluorescence, e.g., by gelbstoff or by phytoplanktonic pigments, has an effect on the accuracy of the absorption determination. For this purpose the fluorescence of the test samples, i.e., of nigrosine and humic acid (see below), was measured in an Aminco-Bowman luminescence spectrometer (excitation of 350 nm; emission of 370–750 nm) and related to the simultaneously occurring Raman scattering. Humic acid is known to fluoresce in the region between 400 and 600 nm, and nigrosine was found to significantly fluoresce between 550 and 650 nm (data not shown). The maximum nigrosine fluorescence at the highest concentration used was in the range of the maximum Raman scatter; i.e., the maximum quantum efficiency of nigrosine fluorescence was less than 0.001. This was estimated by using the Raman absorption coefficient as a reference.[21] Reported quantum efficiencies of natural gelbstoff fluorescence are in the range of 0.005–0.01.[22] In a further test we used an interference filter to provide light of only 447 $\pm$ 12 nm to the PSICAM and measured the total light spectrum when the cavity was filled with a nigrosine solution of a relatively high concentration ($a_{578\,\mathrm{nm}} = 3.2\ \mathrm{m}^{-1}$). No Raman scatter and no fluorescence were detectable. Considering the actual signal-to-noise ratio of the detector, the induced fluorescence yield must be lower than 0.002. Under these conditions and with the solutions used here (the humic acid solutions had concentrations similar to natural gelbstoff concentrations in coastal waters), the influence of fluorescence by the sample can be considered as negligible. The yield for chlorophyll fluorescence is usually higher, between 0.01 and 0.05, and the emis-

sion occurs within a smaller wavelength range (660–720 nm). The influence of chlorophyll fluorescence in the determination of particulate phytoplankton absorption could be significant.

D. Transmission Measurement in the Point-Source Integrating Cavity Absorption Meter

The wall material of the PSICAM is microporous (amorphous); any sample filled into it will penetrate into the wall and will thereby change the reflectivity. Hence, to have constant conditions inside the cavity, it was filled with purified water at least one day before we performed any measurements. The halogen lamp was preburned a few hours when new and switched on 30 min before the measurement to stabilize its output. The spectroradiometer was turned on 1 h before the experiment to stabilize its readings.

To be consistent with previous papers, we follow the nomenclature of Kirk[17] and Leathers *et al.*[18] The term transmission is used for the ratio of two irradiance or radiance measurements within the PSICAM. Simple transmission measurements with the PSICAM are conducted in the following way: The cavity is filled with a reference solution A. We make sure that no bubbles, which would alter the light field inside the cavity, are on the wall of the cavity and especially on the surface of the central sphere. The spectral light intensity for the reference solution, I_0, is determined five to ten times and averaged. The reference solution A is removed, replaced by a sample solution B, and the spectral light intensity for the sample I is determined in the same way as I_0. The transmission T_{AB} is calculated as I/I_0. The overall standard deviation of a regular transmission measurement (Fig. 4), determined by measuring ten times the transmission of purified water against itself using setup R, was lower than 0.15% for all wavelengths (mean of 0.10%). This value is considered to be the minimum standard deviation for all setups of our PSICAM.

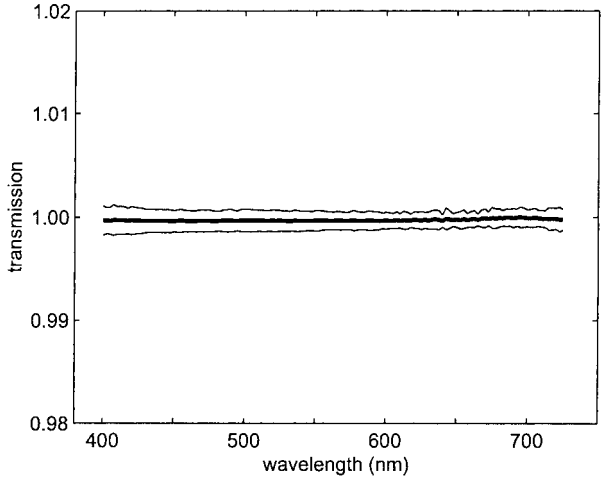

Fig. 4. Mean transmission (thick curve) and standard deviation (thin curves) determined from ten separate transmission measurements of water versus water with the radiance-type detector setup R.

E. Theoretical Considerations

According to Kirk[17] and Leathers *et al.*,[18] the transmission measured in a PSICAM is the ratio of the diffuse reflected irradiance F_0 at the inner wall when the cavity is filled with either sample A or B [Eq. (1)]. It is proportional to the number of times a photon is reflected by the wall, N_C, before it is absorbed either by the wall or by the sample fluid. Hence

$$T_{AB} = \frac{F_0^A}{F_0^B} = \frac{N_C^A}{N_C^B}. \tag{1}$$

N_C is the fraction of photons reaching the wall directly and indirectly by reflection on the wall for one or more times [Eq. (2)]. It depends (1) on the probability P_0 that a photon, coming from the central light source, reaches the wall directly; (2) on the reflectivity of the wall ρ; and (3) on the probability P_s that a photon, which is reflected, will return to the wall. This gives

$$\begin{aligned} N_C &= P_0 + P_0\rho P_s + P_0\rho^2 P_s^2 + \ldots \\ &= P_0 \sum_{n=0}^{\infty} (\rho P_s)^n \\ &= P_0/(1 - \rho P_s). \end{aligned} \tag{2}$$

Therefore

$$T_{AB} = \frac{P_0^A(1 - \rho P_s^B)}{P_0^B(1 - \rho P_s^A)}. \tag{3}$$

P_0 and P_s are related to the radii of the PSICAM $r_0 = r - r_s$ and r, respectively, where r is the inner radius of the cavity and r_s is the radius of the central light source, and to the absorption coefficient a in the following way[17]:

$$P_0(a, r_0) = \exp(-ar_0), \tag{4}$$

$$P_s(a, r) = \frac{1}{2a^2r^2}\,[1 - \exp(-2ar)(2ar + 1)]. \tag{5}$$

Finally, if an unshielded irradiance sensor is used, the transmission in the PSICAM is related to the absorption coefficients a_A and a_B of the two solutions as

$$T_{AB} = \exp[-r_0(a_A - a_B)]\left[\frac{1 - \rho P_s(a_B, r)}{1 - \rho P_s(a_A, r)}\right]. \tag{6}$$

Using a radiance sensor with a narrow field of view or an irradiance sensor that is shielded by a baffle plate will prevent the detection of photons coming directly from the central light source. The first probability P_0 in Eq. (2) would be zero, hence

$$N_C = P_0 \rho P_s + P_0 \rho^2 {P_s}^2 + \ldots = P_0 \sum_{n=1}^{\infty} (\rho P_s)^n = \frac{\rho P_0 P_s}{1 - \rho P_s}. \tag{7}$$

The placing of the baffle destroys the spherical symmetry since it changes r_0 and r for the shielded solid angle. Equation (7) is only an approximation for this more complex situation. It is supposed that the related error for the absorption determination is compensated by the way ρ is determined (see below).

By use of Eqs. (1) and (7), then (4) and (5), the calculation of the transmission changes into

$$T_{AB} = \frac{{P_0}^A (1 - \rho {P_s}^B)}{{P_0}^B (1 - \rho {P_s}^A)} \frac{{P_s}^A}{{P_s}^B} = \exp[-r_0(a_A - a_B)] \left[\frac{1 - \rho P_s(a_B,\ r)}{1 - \rho P_s(a_A,\ r)} \frac{P_s(a_A,\ r)}{P_s(a_B,\ r)} \right]. \tag{8}$$

By solving Eq. (6), the reflectivity ρ for an irradiance sensor setup is

$$\rho = \frac{T_{AB} \exp(-a_B r_0) - \exp(-a_A r_0)}{T_{AB} \exp(-a_B r_0) P_s(a_A,\ r) - \exp(-a_A r_0) P_s(a_B,\ r)}, \tag{9}$$

and, by solving Eq. (8), ρ for a radiance sensor or an irradiance sensor protected by a baffle is

$$\rho = \frac{T_{AB} \exp(-a_B r_0) P_s(a_B,\ r) - \exp(-a_A r_0) P_s(a_A,\ r)}{T_{AB} \exp(-a_B r_0) P_s(a_A,\ r) P_s(a_B,\ r) - \exp(-a_A r_0) P_s(a_B,\ r) P_s(a_A,\ r)}. \tag{10}$$

Hence, if ρ is not known, it can be determined by measuring the transmission of two solutions with known absorption coefficients using Eq. (9) or (10).

F. Determination of the Effective Wall Reflectivity ρ and Calculation of the Absorption

The error for absorption determination in a PSICAM is related mainly to the error in determining the inner radius r, the reflectivity of the PSICAM ρ, and the transmission determination in the PSICAM.[2,18] The transmission measurement is further influenced by the stability of the light source and the spectroradiometer response (see above). From these errors the error related to ρ has the strongest influence: A 1% error in ρ leads to >10% error in the absorption determination.[2] Hence ρ has to be known with high accuracy. It should preferably be determined using Eq. (9) or (10), respectively, by measuring the transmission of two solutions with known absorption coefficients, rather than measuring the wall reflectivity directly. Determining the effective ρ in this way has the advantage that it will eliminate errors associated with the true ρ of the wall material and with r_0, a_A, a_B, and the water absorption.[18] However, the error of the determination of the absorption coefficient with a photometer, which is needed to determine ρ, influences the error of the absorption determination with the PSICAM.[2,18]

There is no analytical solution for the absorption coefficient $a_{(\lambda)}$ in Eqs. (6) and (8). When ρ is known, $a_{(\lambda)}$ is calculated by solving these equations numerically. This was done by minimizing the least-squares function $G[a_{(\lambda)}]$ for the measured transmission $T_{\exp(\lambda)}$ using a numerically calculated transmission $T_{\mathrm{num}(\lambda)}$:

$$G[a_{(\lambda)}] = \sqrt{[T_{\mathrm{num}(\lambda)} - T_{\exp(\lambda)}]^2}. \tag{11}$$

In practice the reflectivity ρ is determined following the suggestion and description of Leathers *et al.*[18] Therefore the transmission T_{AB} is determined from a sample solution A with an absorption coefficient a_A measured against a reference solution B with an absorption coefficient a_B in the PSICAM. The reference solution consists of purified water. The assumed absorption coefficient spectrum of this purified water is the mean taken from three published pure water absorption coefficient spectra.[20,23,24] These were averaged because each spectrum of ρ determined with each individual water absorption spectrum contained artifacts. These artifacts occur at wavelengths of the major absorption shoulder (~605, 662, and >710 nm) of the water absorption and are related to inaccuracies in the absorption coefficient at these particular wavelengths. Averaging the individual spectra did reduce these artifacts, which are now visible only at wavelengths >700 nm (e.g., see Fig. 9). The sample solutions are prepared from the colored stain nigrosine (Certistain, Merck, Germany), following the suggestions of Kirk.[17] Nigrosine has the advantage of having a considerably high absorption coefficient at all required wavelengths (Fig. 5). A nigrosine stock solution is prepared by dissolving a few crystals of nigrosine in 100 ml of purified water. The absorption of this solution is determined photometrically in a 1 cm cuvette at 578 nm. Sample solutions with an absorption ($a_{578\,\mathrm{nm}}$) between 1 and 10 m^{-1} (on the $\log_n$ scale) are prepared by diluting a few milliliters of the stock solution in ~800 ml of purified water. The spectral absorption coefficients of each nigrosine solution are determined photometrically. The transmission measurements in the PSICAM are

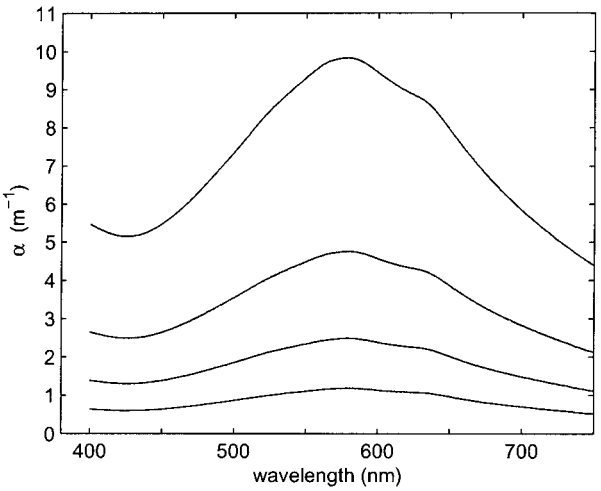

Fig. 5. Spectral absorption coefficient a (m^{-1}) of four nigrosine solutions of different concentration as used to determine the effective wall reflectivity ρ.

conducted in triplicate as described above, except that the PSICAM has to be cleaned after each nigrosine measurement since the stain adsorbs considerably fast on the cavity wall of the PSICAM. Therefore the PSICAM is bleached for 15 min with a 0.1% sodium hypochlorite solution (NaOCl, Riedel de Haën, Germany). Afterwards the bleach is removed from the PSICAM by washing the cavity several times with purified water.

G. Photometric Determination of Absorption and Scattering Coefficients

Photometric measurements were performed in a Lambda 18 dual-beam spectrophotometer (Perkin-Elmer) using either a 1 or 10 cm optical glass cuvette. Purified water was always used as the reference. The water was de-ionized, ultrafiltrated, irradiated with UV using a Milli-Q 185 water purification system (Millipore), and finally stored for 24 h to remove microbubbles. Microbubbles as pure scatterers are no problem for the PSICAM measurements, but they influence the absorption measurements of solutions in photometer cuvettes. The photometer was turned on 1 h before the first measurements. Then, for all measurements, a baseline was performed by inserting a cuvette filled with purified water in the sample beam. The reference beam was left empty, except when we measured solutions with higher attenuation coefficients, and then a 10% neutral-density filter was placed in the reference beam to adjust the sensitivity of the photomultiplier in the photometer. The original performed baseline was checked regularly by measuring purified water of the same temperature (±0.1 °C), and the error of this time-dependent difference in the baseline was determined. This error was lower than the error induced when a second cuvette filled with purified water was used in the reference beam when we performed the baseline, and the sample was measured against this reference cuvette. This is related to small temperature differences (0.1 °C–0.5 °C) between the sample and the reference, since the sample compartment is not temperature controlled. This temperature difference influences the water absorption at a wavelength >700 nm. In this way the absorption from 400 to 750 nm of a specific sample solution was determined against the absorption of purified water with a resolution of 1 nm. At least three separate measurements for each sample were averaged. Considering scattering as negligible, the absorption coefficient a (m^{-1}) was calculated from the measured attenuation A as follows: $a = 2.303A/L$, where L is the path length of the cuvette in meters. The factor of 2.303 converts the logarithm ($\log_{10}$) used in the Lambert–Beer formulation ($A = -\log[T]$) into the natural logarithm. In the same way the scattering coefficient b (m^{-1}) of $BaSO_4$ suspensions was determined in a cuvette with a path length of 1 cm. This was used to test the effects of scattering (see Subsection 3.A). In this case, absorption of $BaSO_4$ was considered as negligible and b was calculated as $b = 2.303A/L$. In addition, the transmission of a $BaSO_4$ suspension was determined when the photometer was equipped with an integrating sphere and the cuvette was placed in front of the entrance of this sphere. This photometric setup for the transmission measurement is used to minimize scattering effects in the determination of absorption in suspensions of planktonic algae.[3]

H. Experimental Design

The performance of the three different PSICAM setups was tested in two ways: (1) the effect of scattering particles suspended in water was determined with suspensions of different concentrations of $BaSO_4$ to test which setup provides the best solution in preventing possible adverse effects by scattering; and (2) the linearity for the absorption determination was examined by determining ρ using a set of solutions with different concentrations of nigrosine. Since ρ is the most sensitive parameter, this exercise should show how stable the PSICAM setup is over a wide range of absorption.

Then the temperature influence on the absorption measurement was tested with setup R by determining ρ at different sample temperatures. Last, the setup performing best, i.e., R, was tested by comparing the absorption by humic acid and $CuSO_4$ solutions determined in the PSICAM with that determined in the photometer.

1. Experiment 1. Determination of Adverse Scattering Effects

The effect of scattering by particles in the PSICAM was tested by measuring the transmission of different $BaSO_4$ suspensions against purified water. $BaSO_4$ has a reflectivity of ~99% and a negligible absorption at the concentrations used (bottle label, Merck, Germany). Four suspensions were prepared with concentrations of 2, 10, 20, and 40 mg/l of a $BaSO_4$ powder (Merck, Germany). A suspension with a concentration of more than 10 mg/l $BaSO_4$ produces a milky suspension that is sufficiently optically

dense. The transmission in the PSICAM of each of these suspensions was determined in triplicate. The scattering coefficient and the transmission of these suspensions were determined in the photometer as described above.

2. Experiment 2. Determination of ρ at Different Sample Absorptions

The reflectivity ρ was determined in triplicate using four different nigrosine solutions of absorption coefficients $a_{578\,\mathrm{nm}}$ between 1 and 10 m^{-1} at 20 °C as described above.

3. Experiment 3. Determination of ρ at Different Sample Temperatures

The reflectivity ρ was determined at two different temperatures (5 °C and 20 °C) of the sample and reference. Therefore nigrosine solutions were prepared at 20 °C as described above and cooled in a refrigerator until a temperature of 5 °C was reached. The exact temperature was determined after the sample and the reference were filled into the PSICAM. Temperature differences between the sample and the reference were less than 0.5 °C. The absorption of each nigrosine solution was determined at 20 °C in the photometer. Changes with temperature were not observed when we measured the absorption of a nigrosine solution photometrically at 10 °C, 20 °C, and 30 °C against purified water of the same temperatures.

The absorption coefficient of pure water at each wavelength is temperature dependent. To calculate the absorption of pure water at different temperatures, spectral values of the temperature coefficient Ψ_T of Buiteveld *et al.*[24] were used, but according to Pegau *et al.*,[25] an offset of 0.0011 m^{-1} $(°\mathrm{C})^{-1}$ applied. The temperature coefficient spectrum used is shown in Fig. 9(a) (below) together with a modeled spectrum of Pegau *et al.*[25] The absorption coefficient at different temperatures is then calculated as

$$a_{T(\lambda)} = a_{20°\mathrm{C}(\lambda)} + (T - 20)\Psi_T. \tag{12}$$

4. Experiment 4. Comparison of the Absorption Determination Using the Point-Source Integrating Cavity Absorption Meter and the Photometer

Absorption coefficients determined in the PSICAM are compared with those determined in the photometer using the best-performing PSICAM setup. At first, five humic acid solutions of different concentrations were prepared by diluting small amounts of humic acid sodium salt (Sigma-Aldrich) in purified water. Second, a $CuSO_4$ solution was prepared by diluting crystals of $CuSO_4 \cdot 5H_2O$ (Merck, Germany) in purified water. The absorption of all solutions was determined in triplicate in a photometer using a 10 cm cuvette and in the PSICAM.

3. Results and Discussion

A. Influence of Scattering

The influence of scattering on the determination of absorption with the PSICAM was insignificant. The four $BaSO_4$ suspensions of 2, 10, 20, and 40 mg/l had photometrically determined scattering coefficients between 2 and 30 m^{-1} [Fig. 6(a)]. The scattering coefficient increased with the $BaSO_4$ concentration and is slightly wavelength dependent, showing higher values at smaller wavelengths. The transmission of these suspensions measured in front of an integrating sphere in the photometer, when the backwards and sidewards scattered photons are lost, decreased with increasing $BaSO_4$ concentration and ranged from 99.99% to 96.90% [Fig. 6(b)]. The transmission was wavelength dependent for suspensions with higher $BaSO_4$ concentrations (20 and 40 mg/l). The suspension with the lowest $BaSO_4$ concentration (2 mg/l) had a mean transmission of 99.94%.

The transmission (as defined above), measured with the three different PSICAM setups, was between 99.20% and 100.60% (Fig. 7). A wavelength dependence could not be observed, except for the sus-

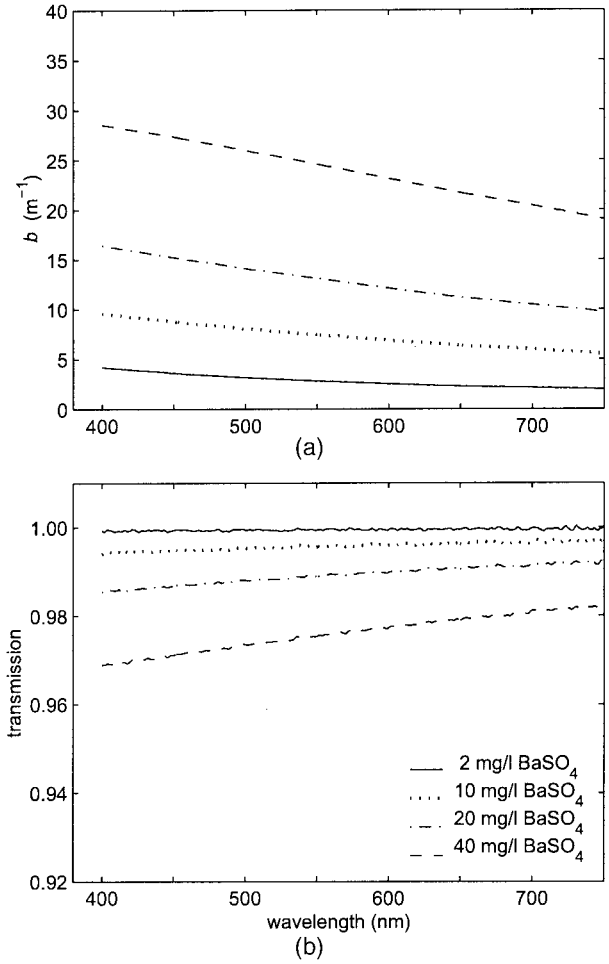

Fig. 6. Photometric measurements of $BaSO_4$ suspensions of different concentrations. (a) Spectral scattering coefficient b (m^{-1}). (b) Spectral transmission measured in front of an integrating sphere.

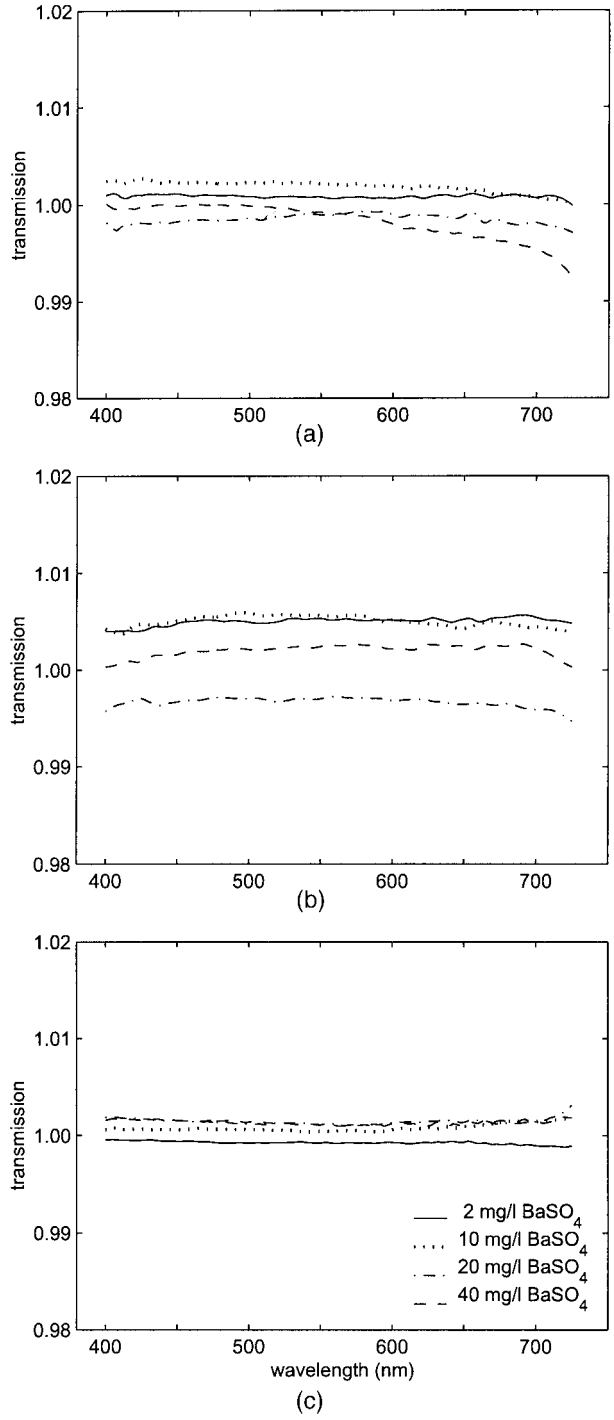

Fig. 7. Spectral transmission of the $BaSO_4$ suspensions measured with the different PSICAM setups: (a) Irradiance setup I, (b) irradiance plus baffle setup IS, (c) radiance setup R. The corresponding scattering coefficients b (m^{-1}) are shown in Fig. 6.

pension with the highest $BaSO_4$ concentration (40 mg/l) when measured with setup I. The mean standard deviation for all measurements ($n = 36$) was ~0.26%, i.e., approximately twice that of the minimum mean standard deviation of the determination (0.10%) in the PSICAM (see above). With the two irradiance setups I and IS, the transmission did not vary with the suspension's $BaSO_4$ concentration but scattered around the theoretical value of 100% (I, 99.2%–100.3%; IS, 99.4%–100.6%). When we used setup R, the transmission increased with increasing $BaSO_4$ concentrations (variation of 99.9%–100.3%). However, for all measurements with the radiance sensor, the observed mean standard deviation (0.10%) was approximately the same as the minimum standard deviation for repeated determinations (0.15%; mean, 0.10%; see above).

Compared with natural samples, the scattering coefficients of the $BaSO_4$ suspensions used were very high, especially for the highest concentrations that were not transparent but opaque. For all $BaSO_4$ concentrations, measurements with the three PSICAM setups perform better than measurements with a photometer equipped with an integrating sphere. The photometer method might provide more exact values only at low sample scattering and high sample absorption. However, the theoretical mean optical path length of our PSICAM is much larger (up to 3 m)[17]; hence the signal differences between the sample and the reference (I versus I_0) are larger. At low sample absorption, as found with natural samples, the percentage error due to scattering effects would be much lower than that of the photometric method. At natural conditions the PSICAM would perform better than the photometric method, especially for samples that have a comparably high scattering coefficient, e.g., in coastal waters. In this case the difference between the three PSICAM setups are small, but setup R shows a lower variation than the two other setups and hence would provide a more exact determination. Setup IS has a practical disadvantage, since the baffle plate prevents the observation of any air bubbles sitting on the central light source. Bubbles alter the homogeneity of the light field in the cavity and influence the transmission determination, and thus have to be checked. The higher variation in the transmission measurements [Fig. 7(b)] might be due to the existence of more or fewer bubbles on the central sphere during these measurements.

B. Determining the Linearity Range of the Point-Source Integrating Cavity Absorption Meter Absorption Measurements

The effective reflectivity ρ determined with setup I ranged from 0.967 at 400 nm to 0.987 at 700 nm [Fig. 8(a)]. ρ, when determined with the highest nigrosine concentration, was significantly higher than that determined with the other three concentrations. Using setup IS, the variation in the reflectivity spectra was reduced and ρ was between 0.967 at 400 nm and 0.981 at 700 nm [Fig. 8(b)]. The reflectivity determined with the lowest nigrosine concentration differed at wavelengths smaller than 500 nm and greater than 700 nm, whereas the reflectivity determined with the highest nigrosine concentration differed between 500 and 700 nm from that determined with the other three concentrations, respectively. By use of setup R, this variation was further reduced. Only the reflectivity spectrum determined with the

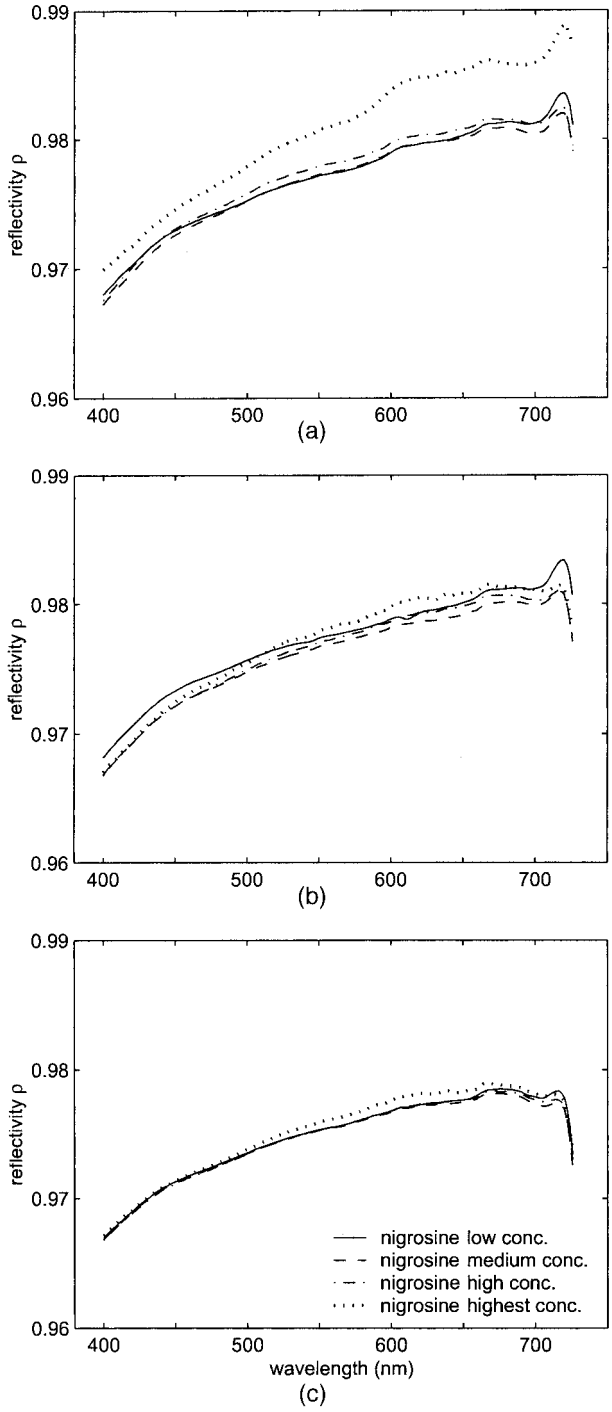

Fig. 8. Spectral reflectivity ρ determined with four different nigrosine solutions using the three different PSICAM setups: (a) Irradiance setup I, (b) irradiance plus baffle setup IS, (c) radiance setup R. The approximate spectral absorption of each solution is shown in Fig. 5.

highest nigrosine concentration differed slightly between 500 and 700 nm from the other three reflectivity spectra determined [Fig. 8(c)]. The reflectivity ranged from 0.967 at 400 nm to 0.978 at 700 nm.

The measured reflectivity spectra are similar to the known spectrum of the wall material but show a weak wavelength dependency with lower reflectivity at shorter wavelengths. For setup I it was expected that the reflectivity would differ at higher sample absorption because the detector will collect relatively more photons coming directly from the central light source. This is visible in a higher reflectivity measured with the highest nigrosine concentration for this setup. At lower nigrosine concentrations (lower absorptions), the reflectivity is relatively stable. When a baffle was used to prevent photons from entering the detector directly from the central light source, as in setup IS, the reflectivity determined with the highest nigrosine concentration was only slightly higher than the reflectivities determined with the other three nigrosine solutions. However, in this case the reflectivity determined with the lowest nigrosine concentration differed clearly. When we used a radiance sensor, as in setup R, the determined reflectivities were lower than those obtained with the other setups but were very similar for the three lowest nigrosine concentrations [Fig. 8(c)].

When the values for the highest nigrosine concentration are excluded, the maximal standard deviations of all wavelengths are 0.14%, 0.33%, and 0.06% and the mean standard deviations are 0.041%, 0.062%, and 0.011% for setup I, IS, and R, respectively. Considering that a 1% error in ρ results in an error of ~15% for the absorption determination (extrapolated from data of Lerebourg *et al.*[2]), the maximal error in absorption, induced by an error in the determination of ρ, would be 2.2%, 4.5%, and 0.9%, respectively. This means that setup R would provide the most exact determination, with a linear response for absorptions between 0.1 and 5 m^{-1}. Since this setup also performed best in excluding the effects of scattering, it was considered as the setup of choice for the following comparisons.

1. *Temperature Influence on* ρ

One advantage of a PSICAM is the high sensitivity due to a relatively long optical path length, which would allow us to determine very low absorption coefficients of untreated seawater samples. It is preferred that these samples could be measured directly after sampling and at ambient temperature. Therefore the temperature dependence of the ρ determination was examined, which should show any error produced by temperature-related physical changes in the PSICAM. ρ was determined with nigrosine solutions at temperatures of 5 °C and 20 °C (Fig. 9) and decreased little with decreasing temperature. The maximum difference of 0.07% was found between 400 and 440 nm. This difference can partly be explained by small errors in the temperature coefficient Ψ_T used to determine the pure water absorption at each temperature. Changing the offset of the data of Buiteveld *et al.*[24] from 0.0011 to 0.0014 m^{-1} $(°C)^{-1}$ and setting Ψ_T to 0 at wavelengths below 500 nm, which is similar to the data for Ψ_T measured by Trabjerg and Højerslev[26] [see Fig. 9(a)], significantly reduced the variability of the determined reflectivity to a difference at a maximum of 0.04% [Fig. 9(b)]. The observed

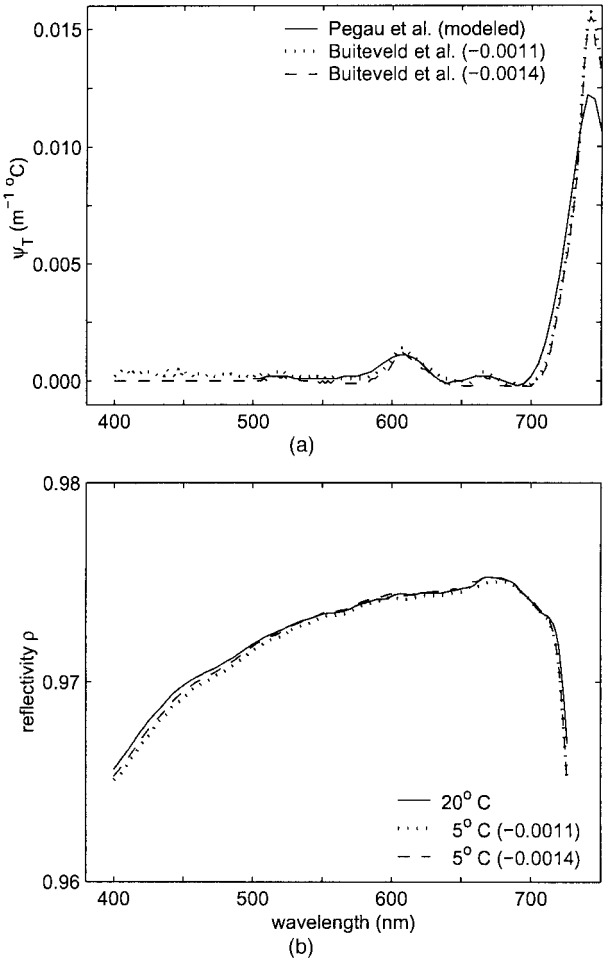

Fig. 9. (a) Different estimates for the spectral temperature coefficient Ψ_T of the absorption of pure water. The spectral data of Buiteveld *et al.*[24] minus an offset (shown in parentheses) were used to calculate absorption of water at different temperatures. An additional modeled spectrum is shown.[25] (b) Spectral reflectivity ρ determined at different temperatures. Spectra at 5 °C are shown for the calculation of pure water absorption with a different offset for Ψ_T (see above).

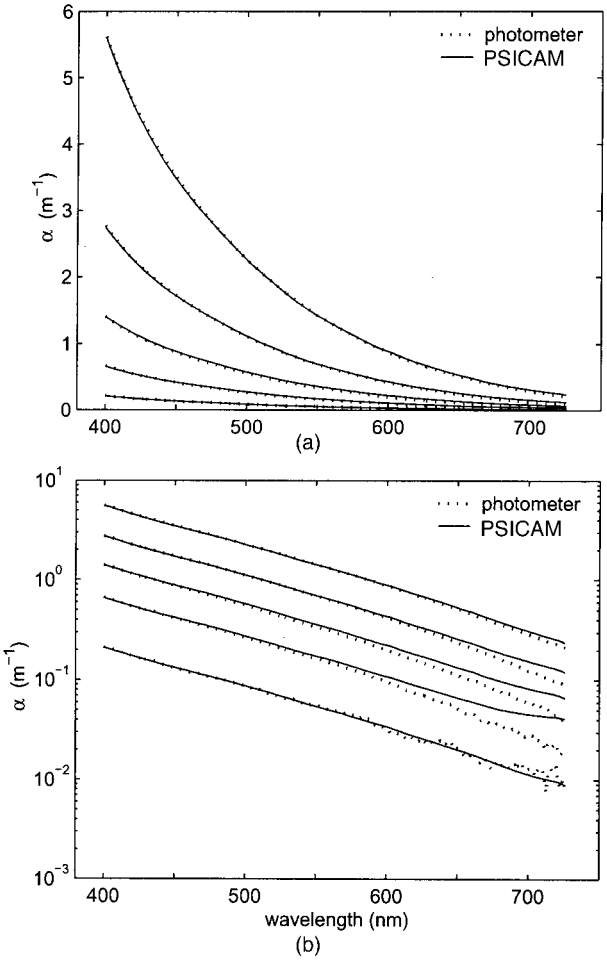

Fig. 10. Spectral absorption coefficients a (m^{-1}) of humic acid solutions of four different concentrations determined with the photometer (dotted curves) and the PSICAM (solid curves). (a) Linear scale. (b) Semilogarithmic scale.

variation of ρ at different temperatures is very small and would induce an error at a maximum of 0.6% for the absorption determination. Hence using an appropriate temperature coefficient for pure water absorption allows us to measure the sample and the reference at different temperatures. Finally the temperature for each sample did not have to be the same, but it has to be known for a subsequent calculation of the absorption coefficient.

2. *Absorption Determined with the Point-Source Integrating Cavity Absorption Meter and the Photometer*

The absorption determined with the PSICAM was compared with that measured with a photometer over a wide range of absorptions using humic acid and $CuSO_4$ solutions (Figs. 10 and 11). A humic acid solution has similar optical characteristics as those of natural colored dissolved organic matter (gelbstoff). It has little absorption at longer wavelengths (>600 nm); this is why a $CuSO_4$ solution was used for this spectral region in a second comparison. It was considered that, at low absorption coefficients, photometric measurements are less accurate than PSICAM measurements due to a much smaller optical path length. Hence data of low absorptions (<0.1 m^{-1}) were not used for the following comparisons. The humic acid solutions had absorption coefficients ranging from 0.2 to 5 m^{-1} at 412 nm (Fig. 10). This is similar to the absorption coefficients of gelbstoff found in waters of the German Bight ranging from the clear central North Sea to the turbid Elbe River. The mean difference for all humic acid solutions in the spectral range of 400–600 nm was 2.35% (Table 1), and the averaged difference at 412 nm was 0.71% ($n = 5$) (see Table 1). The averaged maximal difference ($n = 5$) for this range was 7.65%, and these maxima were found always at longer wavelengths, i.e., with low absorption values. For the $CuSO_4$ solution (Fig. 11), which had an absorption of ~0.3 m^{-1} at 600 nm, the mean error was 1.64% (maximum of 5.74%) at wavelengths of 600–730 nm. Again the

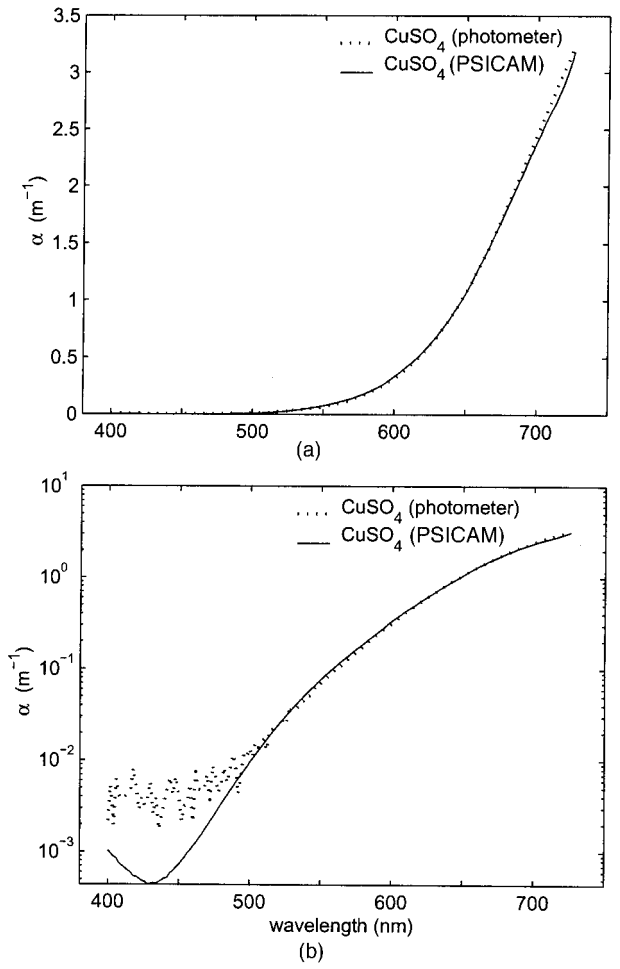

Fig. 11. Spectral absorption coefficients a (m^{-1}) of a $CuSO_4$ solution determined with the photometer (dotted curves) and the PSICAM (solid curves). (a) Linear scale. (b) semilogarithmic scale.

highest difference was found at the lowest absorption values (600 nm). The error for the determination of a with the PSICAM depends only on the error for ρ and for the transmission T, since all other errors (r, r_s, a_A, a_B, water absorption) are included in the error of ρ due to its type of determination.[18] The observed mean differences in a (1.64%–2.35%) are slightly higher than the maximal error for a caused by these two errors (±1.05% = 0.9% + 0.15%). This 1.05% error is basically the error if this comparison were based on the nigrosine solutions used to determine ρ. These solutions had absorption coefficients between 0.5 and 10 m^{-1}. Since the maximum difference was found at relatively low absorption values (<0.3 m^{-1}), it is most likely that the error of the photometric determination causes the relatively high differences at low absorption.

4. Conclusions

The PSICAM prototype tested with different collector configurations showed the theoretically predicted low error caused by scattering over a broad range of scattering coefficients. This error will be insignificant for the range of optical properties found in oceanic and most coastal waters. The temperature influence on the absorption determination was weak; this makes it possible to determine the effective ρ of the PSICAM under constant laboratory conditions at room temperature and then to use the PSICAM later at various ambient temperatures under field conditions. The PSICAM tested provides a linear response for absorption coefficients at least from 0.1 to ~5 m^{-1}. It was constructed to work with water from the North Sea and was found not to be sensitive enough to work in the clearest oceanic waters.[27] However, the sensitivity can be increased by enlarging the diameter of the cavity. Nevertheless it is more sensitive than a regular photometer for the determination of gelbstoff absorption of natural waters.

The PSICAM equipped with a radiance collector showed the best performance: The overall error, caused by scattering, of the transmission measurement and of the ρ determination was smaller than for the other two setups. The mean differences between measurements with this setup and the photometric method were below 4.5% and less than 2.3% at higher absorption coefficients. Higher differences at low absorption were most likely due to the lower sensitivity of the photometric determination.

Future work will examine the influence of chlorophyll fluorescence on the absorption determination

Table 1. Relative Differences in Absorption Determined with the PSICAM to that Determined with the Photometer[a]

(%)	412 nm	500 nm	600 nm	700 nm	Maximum (λ)	$Mean_{400–600\ nm}$
HA1 (0.2 m^{-1})	1.49	0.23	3.76	n.d.[b]	6.62 (582 nm)	1.80
HA2 (0.6 m^{-1})	0.68	3.29	12.74	n.d.	12.74 (600 nm)	4.06
HA3 (1.2 m^{-1})	0.62	4.33	13.08	n.d.	13.08 (600 nm)	4.47
HA4 (2.4 m^{-1})	0.45	0.67	3.87	n.d.	3.87 (600 nm)	0.97
HA5 (5.0 m^{-1})	0.32	0.22	1.95	n.d.	1.95 (600 nm)	0.46
Mean (all HA)	0.71	1.75	7.08	n.d.	7.65	2.35
$CuSO_4$	n.d.	n.d.	5.74	2.30	5.74 (600 nm)[c]	1.64[d]

[a]Data are shown for different wavelengths and for one $CuSO_4$ solution and five humic acid solutions of increasing concentration (HA1 to HA5) with $a_{412\ nm}$ between 0.2 and 5.0 m^{-1}. See Figs. 10 and 11 for the corresponding absorption spectra. In addition, the maximum and the mean difference for the respective wavelength range is shown together with the corresponding wavelength of the maximum.
[b]Values not determined because it is assumed that the photometric determination is not sufficiently sensitive at very low absorption.
[c]Maximum difference for data between 600 and 700 nm.
[d]Mean difference for data between 600 and 700 nm.

with the PSICAM. Furthermore, the PSICAM measurements will be compared with other methods for the determination of absorption by particulate matter including the bleaching method to measure the part of the particulate absorption caused by phytoplankton pigments.

We thank Helmut Schiller for his help with the algorithms and two anonymous reviewers for their valuable comments on the paper. This work was supported by the MERIS Application and Regional Products Project (07 UFE 16/1) of the German Federal Ministry for Education and Research.

References and Notes

1. W. S. Pegau, J. S. Cleveland, W. Doss, C. D. Kennedy, R. A. Maffione, J. L. Mueller, R. Stone, C. C. Trees, A. D. Weidemann, W. H. Wells, and J. R. V. Zaneveld, "A comparison of methods for the measurements of the absorption coefficient in natural waters," J. Geophys. Res. **100,** 13201–13220 (1995).
2. C. J.-Y. Lerebourg, D. A. Pilgrim, G. D. Ludbrook, and R. Neal, "Development of a point source integrating cavity absorption meter," J. Opt. **4,** S56–S65 (2002).
3. J. T. O. Kirk, *Light and Photosynthesis in Aquatic Ecosystems,* 2nd ed. (Cambridge U. Press, 1994).
4. S. Tassan and G. M. Ferrari, "An alternative approach to absorption measurements of aquatic particles retained on filters," Limnol. Oceanogr. **40,** 1358–1368 (1995).
5. C. S. Yentsch, "Measurements of visible light absorption by particulate matter in the ocean," Limnol. Oceanogr. **7,** 207–217 (1962).
6. J. T. O. Kirk, "Spectral absorption properties of natural waters: contribution of the soluble and particulate fractions to light absorption in some inland waters of southeastern Australia," Aust. J. Mar. Freshwater Res. **31,** 287–296 (1980).
7. H. Maske and H. Haardt, "Quantitative in vivo absorption spectra of phytoplankton: detrital absorption and comparison with fluorescence excitation spectra," Limnol. Oceanogr. **32,** 620–633 (1987).
8. M. Babin and D. Stramski, "Light absorption by aquatic particles in the near-infrared spectral region," Limnol. Oceanogr. **47,** 911–915 (2002).
9. C. S. Roesler, "Theoretical and experimental approaches to improve the accuracy of particulate absorption coefficients derived from quantitative filter technique," Limnol. Oceanogr. **43,** 1649–1660 (1998).
10. B. G. Mitchell and D. A. Kiefer, "Determination of absorption and fluorescence excitation spectra for phytoplankton," in *Marine Phytoplankton and Productivity,* O. Holm-Hansen, ed. (Springer, 1984), pp. 157–169.
11. B. G. Mitchell and D. A. Kiefer, "Chlorophyll *a* specific absorption and fluorescence excitation spectra for light-limited phytoplankton," Deep-Sea Res. **35,** 639–663 (1988).
12. J. S. Cleveland and A. D. Weidemann, "Quantifying absorption by aquatic particles: a multiple scattering correction for glass-fiber filters," Limnol. Oceanogr. **38,** 1321–1327 (1993).
13. P. Elterman, "Integrating cavity spectroscopy," Appl. Opt. **9,** 2140–2142 (1970).
14. E. S. Fry and G. Kattawar, "Measurement of the absorption coefficient of ocean water using isotropic illumination," Proc. SPIE **925,** 142–148 (1988).
15. E. S. Fry, G. Kattawar, and R. M. Pope, "Integrating cavity absorption meter," Appl. Opt. **31,** 2055–2065 (1992).
16. J. T. O. Kirk, "Modeling the performance of an integrating-cavity absorption meter: theory and calculations for a spherical cavity," Appl. Opt. **34,** 4397–4408 (1995).
17. J. T. O. Kirk, "Point-source integrating-cavity absorption meter: theoretical principles and numerical modeling," Appl. Opt. **36,** 6123–6128 (1997).
18. R. A. Leathers, T. V. Downes, and C. O. Davis, "Analysis of a point-source integrating-cavity absorption meter," Appl. Opt. **39,** 6118–6127 (2000).
19. J. T. O. Kirk, Kirk Marine Optics, Murrumbateman, Australia (personal communication, 1999).
20. R. M. Pope and E. S. Fry, "Absorption spectrum (380–700 nm) of pure water. II. Integrating cavity measurement," Appl. Opt. **36,** 8710–8723 (1997).
21. B. R. Marshall and R. C. Smith, "Raman scattering and in-water ocean optical properties," Appl. Opt. **29,** 71–84 (1990).
22. C. D. Mobley, *Light and Water. Radiative Transfer in Natural Waters* (Academic, 1994).
23. R. M. Pope, "Optical absorption of pure water and seawater using the integrating cavity absorption meter," Ph.D. dissertation (Texas A&M University, College Station, Texas, 1993).
24. H. Buiteveld, J. M. H. Hakvoort, and M. Donze, "The optical properties of pure water," Proc. SPIE **2258,** 174–183 (1994).
25. W. S. Pegau, D. Gray, and J. R. V. Zaneveld, "Absorption and attenuation of visible and near-infrared light in water: dependence on temperature and salinity," Appl. Opt. **36,** 6035–6046 (1997).
26. I. Trabjerg and N. K. Højerslev, "Temperature influence on light absorption by fresh water and seawater in the visible and near-infrared spectrum," Appl. Opt. **35,** 2653–2658 (1996).
27. R. Röttgers, personal observation.